

RESEARCH

Open Access



TaWI12 may be involved in pistillody and leaf cracking in wheat

Yuhuan Guo^{1,2}, Yan Zhang², Yuhao Li², Yichao Wu², Mingli Liao², Zhengsong Peng³, Zaijun Yang^{2*} and Yonghong Zhou^{1*}

Abstract

TaWI12 is a member of the wound-induced (WI) protein family, which has been implicated in plant stress responses and developmental processes. Wheat (*Triticum aestivum* L.) is a crucial staple crop upon which human sustenance relies. Consequently, investigating the developmental mechanisms of pistils and stamens in wheat is profoundly significant for enhancing wheat characteristics and boosting productivity. In this study, we cloned *TaWI12*, from common wheat and observed a significant resemblance among the three homoeologs of *TaWI12*. The open reading frames (ORFs) of *TaWI12-4A*, *TaWI12-4B* and *TaWI12-4D* were 408 bp, 417 bp and 417 bp, respectively, and encoded 135, 138 and 138 amino acids, respectively. The phylogenetic tree revealed a high degree of homology between the protein sequences of TaWI12 and the wound-induced proteins of *Hordeum vulgare* (KAI4994568) and *Aegilops tauschii* (XP_020196548). To clarify the characteristics and functions of *TaWI12* homoeologs, we obtained transgenic positive plants of *Arabidopsis thaliana* and observed significant filament shortening and decrease. Simultaneously, we used the CRISPR/Cas9 system to generate mutant plants via the modification of three homoeologs of *TaWI12* in wheat. We noticed two distinct phenotypic differences in the knockout mutant. First, we observed the different degrees of homologous conversion of stamens to pistils in the single mutant *TaWI12-4D*. Second, we observed leaf cracking in both the single mutant *TaWI12-4A* and the double mutants *TaWI12-4A* and *TaWI12-4D*. Our findings further revealed that *TaWI12* plays an important role in flower development, which is important for revealing the molecular mechanisms of pistil and stamen development in wheat and has important application value for high-yield wheat breeding.

Highlights

- *TaWI12* overexpression in *Arabidopsis* caused filament shortening and decreasing.
- 1 bp insertion or deletion in upstream of ATG increased the expression of *TaWI12* and caused varying degrees of pistillody traits in wheat.
- Utilizing CRISPR/Cas9 technology to modify *TaWI12* in the coding region caused varying degrees of leaf cracking in wheat.

Keywords Wheat, *TaWI12*, Flower development, Pistillody, Filament shortening

*Correspondence:

Zaijun Yang
yangzaijun1@126.com
Yonghong Zhou
zhouyh@sicau.edu.cn

¹Triticeae Research Institute, Sichuan Agricultural University, Chengdu 611130, China

²Key Laboratory of Southwest China Wildlife Resource Conservation (ministry of education), College of Life Science, China West Normal University, Nanchong 637002, China

³School of Agricultural Science, Xichang University, Xichang 615000, China



© The Author(s) 2025. **Open Access** This article is licensed under a Creative Commons Attribution-NonCommercial-NoDerivatives 4.0 International License, which permits any non-commercial use, sharing, distribution and reproduction in any medium or format, as long as you give appropriate credit to the original author(s) and the source, provide a link to the Creative Commons licence, and indicate if you modified the licensed material. You do not have permission under this licence to share adapted material derived from this article or parts of it. The images or other third party material in this article are included in the article's Creative Commons licence, unless indicated otherwise in a credit line to the material. If material is not included in the article's Creative Commons licence and your intended use is not permitted by statutory regulation or exceeds the permitted use, you will need to obtain permission directly from the copyright holder. To view a copy of this licence, visit <http://creativecommons.org/licenses/by-nc-nd/4.0/>.

Introduction

Allohexaploid bread wheat (AABBDD) is a monocot and belongs to the order *Poales* [1]. It is widely regarded as the primary source of plant-based protein in human nutrition and contains an abundance of essential nutrients, including proteins, fats, carbohydrates, dietary fibers, sugars, vitamins, and micronutrients [2]. The versatility of wheat flour is evident in its capacity to craft a variety of delicious dishes, including bread, cakes, dumplings, and noodles, satisfying people's culinary preferences admirably [3]. Therefore, as one of the foremost food crops worldwide, wheat plays a vital role in ensuring food and nutritional security. According to the United Nations [4], the global population is projected to increase by 30% by 2050, with developing nations expected to face greater food demands than their developed counterparts [5]. Meeting future requirements for food security becomes imperative, necessitating the enhancement of wheat yield-related attributes to address challenges such as population growth, climate change, and the diminishing availability of arable land [6].

Mutants are a form of beneficial germplasm for plant breeding and genetics [7]. In its natural state, common wheat flowers are characterized by one pistil, three stamens and three types of vegetative organs, namely two lodicules, one palea and one lemma. The pistil undergoes development into a single grain following fertilization [8]. Abnormal pistil mutants serve as valuable resources for increasing wheat yield and are categorized into two types [9]. Type I is multi-pistil, which is characterized by the presence of three normal stamens and three fertile pistils, including three-pistil mutants (TP) [10], the three pistils in one floret mutant (12TP) [11], multi-ovary II (DUOII) [12], multi-ovary (MOV) wheat [13], and trigrain wheat [14]. Type II is pistillody, exhibiting varying degrees of homologous transformation of stamens into pistils or pistil-like structures, such as homologous transformation sterility-1 (HTS-1) [15]. Phenotypes with increased pistils or carpels can also be found in rice [16], *Arabidopsis* [17], maize [18], and tomato [19]. HTS-1 is a plant exhibiting pistillody traits that were identified during the cultivation process of the three-pistil near-isogenic line CSTP [15]. Genetic analysis revealed that this trait is governed by two recessive genes. One of these genes is likely located on the 2D chromosome, and is closely linked to the *Pis1* gene, which is responsible for regulating the three-pistil trait. The second recessive gene, *hts-1*, is located within a 7.2 Mb interval on the 4A chromosome [20]. Through RNA-Seq analysis, we discovered a gene called *TaWII2* that is activated in response to wounds. This gene is located inside the *hts-1* localization interval. This gene is expressed at significantly elevated levels in pistillody stamens (PS). Consequently, we hypothesize

that the overexpression of the *TaWII2* gene is crucial in the development of pistillody characteristics in HTS-1.

Wound-induced gene families, including the *win1* and *win2* genes, which are arranged in a closely linked tandem array, were first identified in potato. When potato plants undergo wounding, these two genes show differential organ-specific expression [21]. A study conducted by Yen et al. [22] revealed that the protein WII2, which is produced in response to wounds, tends to accumulate mostly in the cell wall of injured *Mesembryanthemum crystallinum* mesophyll cells. This finding indicates its function in enhancing the composition of the cell wall after injury. Research in soybeans [23], strawberries [24], and rice [25] revealed that *WII2* is involved in the control of biological stress in plants. This engagement is believed to be linked to modifications in the cell wall at the site of wounding and the enhancement of resistance against plant diseases and insect pests. Furthermore, *WII2* is implicated in abiotic stress. In rice [26] and tea plants [27], *WII2* may play a role in regulating cold stress. In *Arabidopsis*, *WII2* (*SAG20*) participates in leaf senescence under ethylene treatment [28]. Despite these advances, there is currently no direct evidence linking *WII2* to the development of flower organs. Interestingly, in *Mesembryanthemum crystallinum*, *WII2* actively participates in reinforcing the cell wall composition at the wound site. Additionally, *WII2* is highly expressed in petals, styles, placenta, and seeds [22]. These observations suggest that *WII2* may have functions beyond wound responses and stress resistance, potentially influencing the development of reproductive structures in plants. Understanding whether *WII2* plays a role in flower morphogenesis is critical, as floral organ development directly impacts reproductive success and, consequently, crop yield. Linking the expression and function of *TaWII2* to floral and reproductive development in wheat could provide insights into mechanisms that regulate key yield traits.

On the basis of the above research, this study further analyzed the function of *TaWII2* in pistil and stamen development in wheat through gene overexpression in *Arabidopsis* and CRISPR/Cas9 gene editing in wheat. The outcomes of this investigation aim to elucidate the function of *TaWII2* in regulating wheat flower development, contribute to a deeper understanding of WII2 family proteins in overseeing plant development, and potentially establish a new theoretical foundation for enhancing wheat resistance and increasing wheat yield through molecular breeding techniques.

Materials and methods

Plant materials

In this study, Seeds of bread wheat (*Triticum aestivum* L.) Chinses Spring (CS), Chuanmai 28 (CM28) and Fielder

were obtained from Sichuan Agricultural University. HTS-1, Chuanmai 28 TP (CM28TP), and Fielder were employed as the plant materials. HTS-1 was selected from the hybrid progeny isogenic of *T. aestivum* cv. CS and three-pistil wheat (TP), whose stamens transformed into pistils or pistil-like structures [15, 20]. CM28TP was selected from the hybrid progeny isogenic of *T. aestivum* cv. CM28 and TP; it has three healthy stamens and three fertile pistils [29]. The seeds of HTS-1 and CM28TP were sown in the experimental field of China West Normal University, Nanchong, Sichuan, China (30°49'N, 106°3'E), in October 2020. Fielder, T₀ and T₁ generation transgenic plants subsequently were grown in pots (10 cm × 20 cm) within a greenhouse under conditions of 16 h of light and 8 h of darkness, maintaining a temperature of 22 °C and a relative humidity of 70% [30]. In accordance with the classification standard of Waddington et al. [31] and considering observations from scanning electron microscopy, young spikes of HTS-1, CM28TP, Fielder, and homozygous Fielder plants edited via CRISPR-Cas9 at the stylar canal closing stage (Developmental score W5.5, spike length 5–6 mm, where pistillody traits began to form), the normal stamens (FS) of Fielder, pistillody stamens (EDPS) and pistils (EDP) of edited homozygous plants at the heading stage were manually dissected for RNA extraction. *Arabidopsis* WT (Col-0, Colombia) and transgenic lines were grown under greenhouse conditions (16-h light/8-h dark cycle, 22 °C, and 70% relative humidity) [32], *Arabidopsis thaliana* was obtained from Arabidopsis Biological Resource Center (ABRC). The leaves of *Arabidopsis* (including Col-0 and transgenic lines) were dissected for DNA and RNA extraction.

DNA, RNA extraction and cDNA synthesis

Total DNA was extracted from the leaves of *Arabidopsis* (including Col-0 and transgenic lines) via the LABGENE™ Plant DNA Isolation Kit (Chengdu Labbio Biotechnology, Chengdu, China), following the manufacturer's instructions. Total RNA was extracted from young spikes of HTS-1, CM28TP, Fielder, homozygous Fielder plants edited via CRISPR-Cas9, EDP, and EDPS of transgenic wheat, FS of Fielder, and leaves of *Arabidopsis* (including Col-0 and transgenic lines) via the Eastep® Super Total RNA Extraction Kit (Promega, Shanghai, China), following the manufacturer's instructions. The integrity and purity of the DNA and RNA were confirmed through 1% RNase-free agarose gel electrophoresis. The DNA and RNA concentrations were calculated via a Nanodrop 2000c spectrophotometer (Thermo Fisher Scientific, MA, USA). First-strand cDNA was synthesized from total RNA according to the instructions of the PrimeScript™ RT reagent kit with gDNA Eraser (Takara, Dalian, China).

Cloning of *TaWI12*

The ORFs sequence of *TaWI12* was cloned from the young spike cDNA of HTS-1 and CM28TP. Since common wheat contains A, B, and D genomes, the specific primers for cloning *TaWI12* from the A (TracesCS4A02G115600), B (TracesCS4B02G188400), and D (TracesCS4D02G189800) genomes were designed with Primer Premier 5.0 (Table 1).

PCR amplification was conducted via the *TaKaRa EX Taq*® DNA polymerase (Takara, Dalian, China) and reactions consisting of 3.0 µL of 10× *EX Taq* Buffer, 2.4 µL of

Table 1 Sequences of primers used in study

Primer name	Forward (5'→3')	Reverse (5'→3')	Purpose
TaWI12-ORF4A	TGGTGGTTCCATGGCC	GCAACTCCTTTGATTCTAGTTTA	Wheat amplification of ORF of the A chromosome primers for PCR
TaWI12-ORF4B	CCTCGAGTGGTGGTTCC	TCATTCGTAGGCTCTGTTGT	Wheat amplification of ORF of the B chromosome primers for PCR
TaWI12-ORF4D	TGGTGGTTCCATGGCC	GCAACTCCTTTGACTTCTAGT TAC	Wheat amplification of ORF of the D chromosome primers for PCR
TaWI12-OE	ATGATGCGCCTCCTCACCG	TTAGATGGCGAGGACGAGGC	<i>Arabidopsis</i> overexpression vector amplification primers for PCR
QaTaWI12	TGGCTAACCATCAGCAGTCCC	AGGCGCAGCAGGAGAACT	<i>Arabidopsis</i> overexpression primers for qRT-PCR
AtGAPDH	GCAACATACGACGAATCA AGAA	CGACACGAGAACTGTAACCCC	<i>Arabidopsis</i> internal reference primers for qRT-PCR
TaU3-F/CeHind-R	GAATTCATCTCACGTTCA ACACC	AAGCGGGAAACGACAATCTG	Wheat gene editing vector detection primers for PCR
TaWI12-4 A	CTTCGGCTCCACCGTCATC	GGCTCTGCCACAGGCACTT	Wheat gene-edited amplification of coding regions of the A chromosome primers for PCR
TaWI12-4B	CTGGCAGGGAAATGGAGG	GACGAGGAGGGGAGGAAGA	Wheat gene-edited amplification of coding regions of the A chromosome primers for PCR
TaWI12-4D	ATGACAGATAAAGACTCGC TAATGG	GGGGGAGAACTGAACTCG	Wheat gene-edited amplification of coding regions of the D chromosome primers for PCR
β-actin	GTCGAACAACCTGGTATTG TGCT	GGATCTTCATTAGATTATCCGT GAG	Wheat internal reference primers for qRT-PCR
QTaWI12	CCACCAACAACGCCAGCG	GGCTCTGCCACAGGCACTT	Wheat overexpression primers for qRT-PCR

dNTP Mixture, 0.36 μL of each primer, 1.0 μL of template cDNA and a certain amount of ddH₂O in a final reaction volume of 25 μL . A T-100 Thermal Cycler (Bio-Rad, Singapore, USA) was used to perform PCR amplification according to the following procedure: predenaturation at 95 °C for 5 min, 35 cycles of denaturation at 95 °C for 30 s, annealing at 60 °C for 32 s, and extension at 72 °C for 60 s; and a final extension at 72 °C for 7 min. After the PCR, 1.5 μL of 10 × loading buffer was added to the PCR product, and the amplified products were electrophoresed on 1.0% agarose gels and then visualized with a Gel Doc 2000 system (Bio-Rad, Singapore, USA). The target DNA bands were recovered and purified from the gels via the E.Z.N.A[®] Gel Extraction Kit (Omega, Georgia, USA). The purified PCR products were subsequently cloned and inserted into the pMD-19T vector (Takara, Dalian, China) and transformed into *E.coli* DH5 α competent cells (Takara, Dalian, China) according to manufacturer's instructions. The transformants were screened on LB agar plates containing ampicillin (100 $\mu\text{g}\cdot\text{mL}^{-1}$) (Meilunbio, Dalian, China). Clones with inserts were identified via blue/white colony selection. Positive clones were subjected to further screening through PCR, and 10 clones from each sample were chosen for sequencing by Sangon Biotech (Sangon, Shanghai, China). Multiple sequence alignment was conducted via DNAMAN 9.0 software.

Bioinformatics analysis of *TaW112* in wheat

The expression specificity of *TaW112* in tissues was examined via WheatOmics 1.0 (<http://202.194.139.32>). The Expasy online tool (<https://web.expasy.org/protparam/>) was used to analyze the physicochemical properties of the proteins, including their molecular weights, theoretical isoelectric points, and hydrophobicity. The secondary structure analysis was accomplished by Novopro and Prabi (https://npsa-pbil.ibcp.fr/cgi-bin/npsa_auto_mat.pl?page=NPSA/npsa_sopma.html). Tertiary structure analysis of the protein was performed via the online software SWISS-MODL (<https://swissmodel.expasy.org/interactive/>). The conserved domain of the *TaW112* protein was predicted via NCBI Conserved Domain Search (CDD, *NCBI Conserved Domain Search* (nih.gov)). Homologous genes of *TaW112* were searched via BLAST from the NCBI database (*BLAST: Basic Local Alignment Search Tool* (nih.gov))), and phylogenetic evolutionary trees were built via the maximum likelihood method in MEGA7.0 software.

Overexpression analysis of *TaW112* in *Arabidopsis*

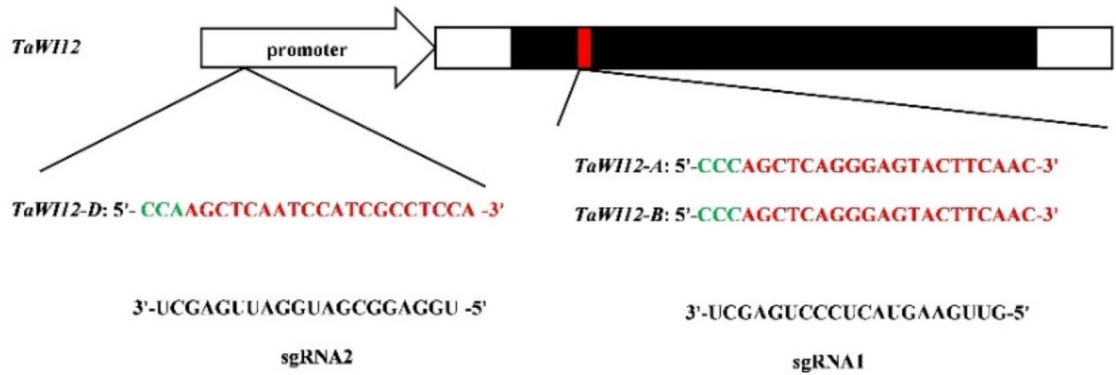
The entire coding sequence (CDS) of *TaW112* (TraesCS4A02G115600) was amplified from the cDNA from the spike of CM28TP as a template with a pair of specific primers *TaW112*-OE (Table 1). The entry clone was obtained via the PentrTM/D-TOPO[™] cloning Kit

(HuaYueYang, Beijing, China), mixed with *E.coli* DH5 α competent cells, cultivated on LB with kanamycin (50 $\mu\text{g}\cdot\text{mL}^{-1}$) (Meilunbio, Dalian, China), and sequenced by Sangon Biotech (Sangon Biotech, Shanghai, China). The recombinant vector D35S::*TaW112*, driven by the CaMV35S promoter, was constructed as follows: 1 μL of entry clone, 1 μL of Destination vector pC1300s (Bio-Vector NTCC Inc., Beijing, China), and 6 μL of TE Buffer (pH 8.0), followed by incubation at 25 °C for 1~2 h; then, 2 μL of LR clonase II enzyme mixture and 1 μL of proteinase K were added, followed by incubation at 37 °C for 10 min. Subsequently, the LR reaction was mixed with *E.coli* DH5 α competent cells, which were cultivated on LB with kanamycin (50 $\mu\text{g}\cdot\text{mL}^{-1}$) and hygromycin (50 $\mu\text{g}\cdot\text{mL}^{-1}$) (Meilunbio, Dalian, China), and sequenced by Sangon Biotech (Sangon, Shanghai, China). The recombinant vector D35S:: *TaW112* was subsequently transformed into *Agrobacterium* GV3101 via the liquid nitrogen freeze-thaw method [33]. This mixture was subsequently transformed into *Arabidopsis thaliana* (Col-0) via the floral dip method [34]. Transgenic plants from the T₀, T₁, and T₂ generations were screened on kanamycin-containing medium (50 $\mu\text{g}\cdot\text{mL}^{-1}$), and successful integration of the transgene was confirmed by PCR. The expression of *TaW112* was verified by qRT-PCR, with *AtGAPDH* (At1g13440) serving as an internal reference [35]. The primers used for amplifying the target gene and *AtGAPDH* are listed in Table 1. Relative quantification of gene expression was performed via the 2^{- $\Delta\Delta\text{Ct}$} method [36]. The error bars represent the standard deviation (SD). Significant differences were statistically analyzed by one-way ANOVA using SPSS 26.0 and GraphPad 8.0 software. All experiments included at least three biological and two technical replicates. Two T₂ seedlings from each transgenic line were grown for further screening of homozygous lines by evaluating the segregation ratio of hygromycin resistance in their progeny at the germination stage. Lines where nearly all progeny seeds (approximately 100%) displayed hygromycin resistance were designated as homozygous. Homozygous T₂ lines were subsequently self-pollinated to produce T₃ seeds, which were used for phenotypic analysis.

Generation of *TaW112* CRISPR/Cas9 mutants in wheat

Using the homogeneous gene sequences of *TaW112* on chromosomes A, B, and D (TraesCS4A02G115600, TraesCS4B02G188400, and TraesCS4D02G189800), we designed 23 bp target points (sgRNA sequences) containing PAM sites (5'-NGG-3') in the exon and promoter regions. sgRNA1 is located on the exons of the *TaW112-4A* and *TaW112-4B* genes, and sgRNA2 is located on the *TaW112-4D* promoter (Fig. 1A). A schematic diagram of the structure of the dual-target editing vector is shown in Fig. 1B. Following genetic transformation

A



B

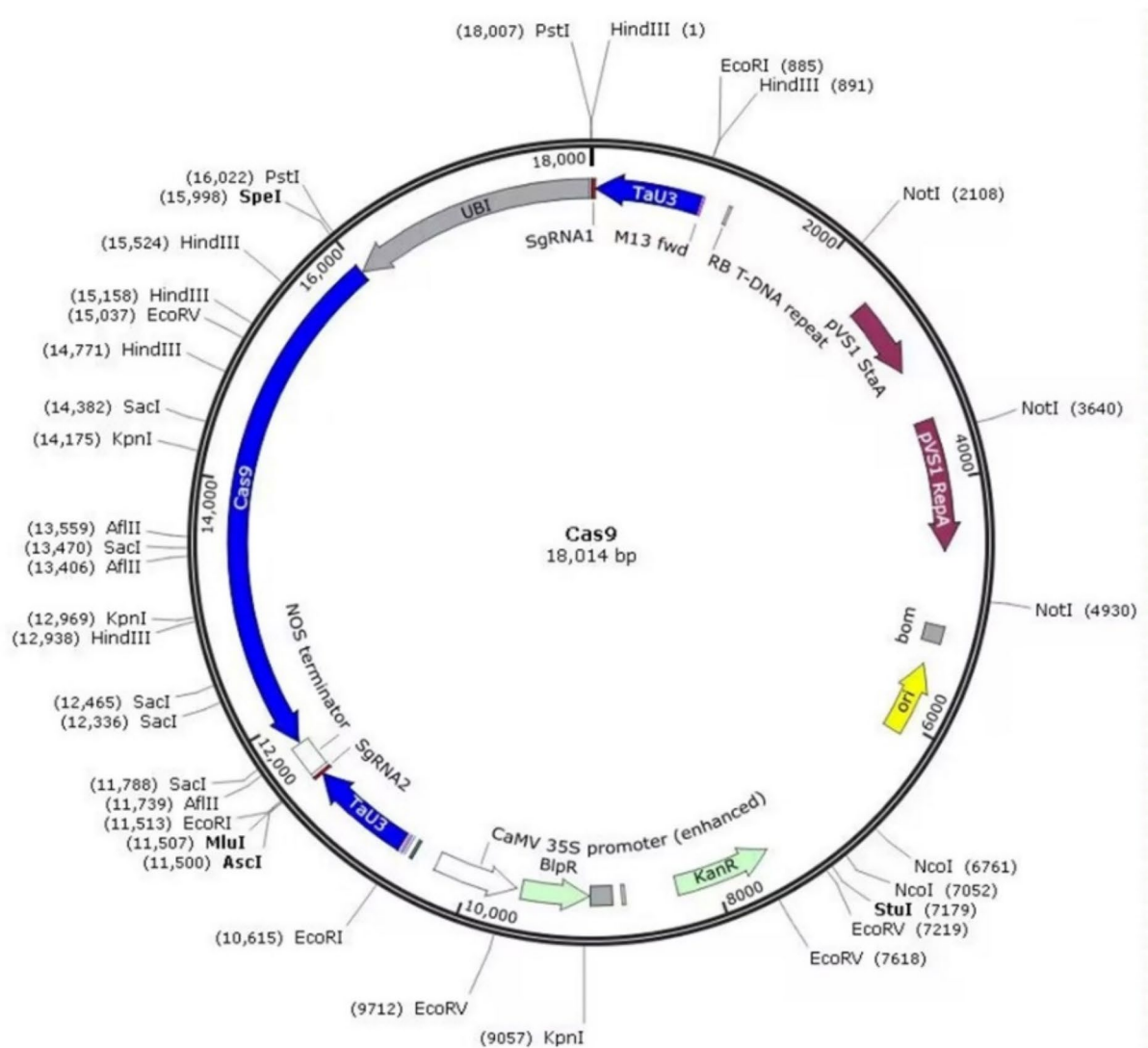


Fig. 1 Schematic diagram of gene editing. **(A)** Schematic diagram of the gene structure of the target site and sgRNA sequence. Note: The green letters and red letters represent the PAM sequences and the sgRNA sequences, respectively. **(B)** Structure of the dual-target editing vector

of *Agrobacterium* species [37], seedlings of transgenic plants were generated. To screen for edit-positive plants, the vector-specific primers TaU3-F and CeHind-R were used for PCR detection of T₀ generation transgenic wheat. Specific mutation analysis of the T₀ generation was conducted on the selected CRISPR/Cas9-positive plants via TA cloning and sequencing of the *TaW112* gene. The T₁ generation was obtained via self-fertilization of the T₀ generation. The *TaW112* gene from T₁ generation plants was subsequently cloned, and 10 positive clones were selected for sequencing. If the 10 clones exhibited the same mutation site, we considered that we obtained homozygous CRISPR/Cas9 mutant plants.

qRT-PCR was used to analyze the expression of *TaW112* in young spikes of Fielder (including both wild-type and edited homozygous plants), EDP, EDPS, and FS with β -Actin (AB181991) used as the internal reference [38]. The primers for the target gene and β -Actin are provided in Table 1.

Phenotypic identification

Ten individual plants were randomly selected from each homozygous edited wheat line and transgenic *Arabidopsis* line for phenotypic analysis. The morphological structures of floral organs in wheat and *Arabidopsis* were observed via a SZX9-3122 stereomicroscope (Olympus, Tokyo, Japan), and images of the plants, spikes and leaves were acquired via an EOS 80D camera (Canon, China).

Results

Isolation and sequence analysis of homoeolog genes of *TaW112* on chromosomes 4A, 4B and 4D

The cDNA derived from reverse transcription of total RNA extracted from young spikes of CM28TP and HTS-1 served as a template for PCR amplification. Three homologous genes of *TaW112*, namely *TaW112-4 A*, *TaW112-4B*, and *TaW112-4D*, were extracted from chromosomes 4A, 4B, and 4D, respectively. The ORFs of the three homologous genes were 408 bp, 417 bp and 417 bp (Fig. 2A), encoding 135, 138, and 138 amino acid residues, respectively. The amino acid sequence similarity was 95.17% (Fig. 2B). Additionally, the sequences of the three homologous genes are identical in both CM28TP and HTS-1.

We identified potential orthologs of *TaW112* by comparing its amino acid sequence with those of various plant species via NCBI. A phylogenetic tree of the WI protein was subsequently constructed through the application of the maximum likelihood method to a multiple alignment of amino acid sequences. Within the phylogenetic tree, the 16 WI proteins were categorized into two clusters. Notably, *TaW112-4A*, *TaW112-4B*, *TaW112-4D* and several putative orthologs from *Hordeum vulgare*, *Aegilops tauschil subsp. strangulate*, *Brachypodium*

distachyon, *Lolium perenne*, and *Lolium rigidum* were grouped together in one cluster (Fig. 2C). Further analysis through BLAST revealed that the amino acid sequence of *TaW112* exhibited 96.3% identity with HvWI (*Hordeum vulgare*, XP_020196548) and 93.48% identity with AsWI (*Aegilops tauschil subsp. Strangulate*, KAI4994568).

Bioinformatics analysis of the *TaW112* protein

The computations of various physical and chemical parameters, including the number of amino acids, molecular weight, theoretical pI, total number of negatively charged residues (Asp + Glu), total number of positively charged residues (Arg + Lys), formula, instability index (II), aliphatic index and grand average of hydropathicity (GRAVY), for the *TaW112-4A*, *TaW112-4B*, and *TaW112-4D* proteins are listed in Table 2.

All three proteins were categorized as unstable and assumed to be hydrophobic proteins (Fig. 3A). The ratios of the secondary structure compositions of the *TaW112-4A*, *TaW112-4B*, and *TaW112-4D* proteins are listed in Table 3, and the secondary structures of which are shown in Fig. 3B.

The tertiary structures of the *TaW112-4A*, *TaW112-4B*, and *TaW112-4D* proteins are shown in Fig. 3C. As shown in Fig. 3C, the tertiary structures of the *TaW112-4B* and *TaW112-4D* proteins were highly similar. The prediction of conserved structural domains verified that the *TaW112-4A*, *TaW112-4B* and *TaW112-4D* proteins belong to the WI12 superfamily (Fig. 3D).

Phenotypic analysis of *TaW112* overexpressing *Arabidopsis*

To investigate the potential role of *TaW112*, an overexpression vector was constructed and introduced into *Arabidopsis* through the floral dip method [34]. Screening of transgenic plants was conducted using hygromycin (50 $\mu\text{g}\cdot\text{mL}^{-1}$), and positive lines were further confirmed via PCR analysis (Fig. 4A). Among the 15 T₁ generation plants tested, 7 individuals (plants 1, 2, 6, 7, 8, 12, and 15) were confirmed as positive transgenic lines. The transcript levels of the *TaW112* gene were assessed via qRT-PCR. The results revealed a significant increase in the expression levels in the transgenic plants compared with those in the wild type (Col-0) plants (Fig. 4B). The flower phenotypes of homozygosity T₃ generation transgenic plants before and during pollination were subsequently examined via stereomicroscopy, revealing noticeable anther filament shortening and a number of filaments varying from 2 to 6 compared with those of Col-0 plants (Fig. 4C). These observations suggest that overexpression of *TaW112* in *Arabidopsis* induces notable alterations in stamen development, providing insights into the potential roles of this gene. However, we emphasize that these findings primarily reflect the effects of *TaW112* overexpression in the *Arabidopsis* system and may not fully

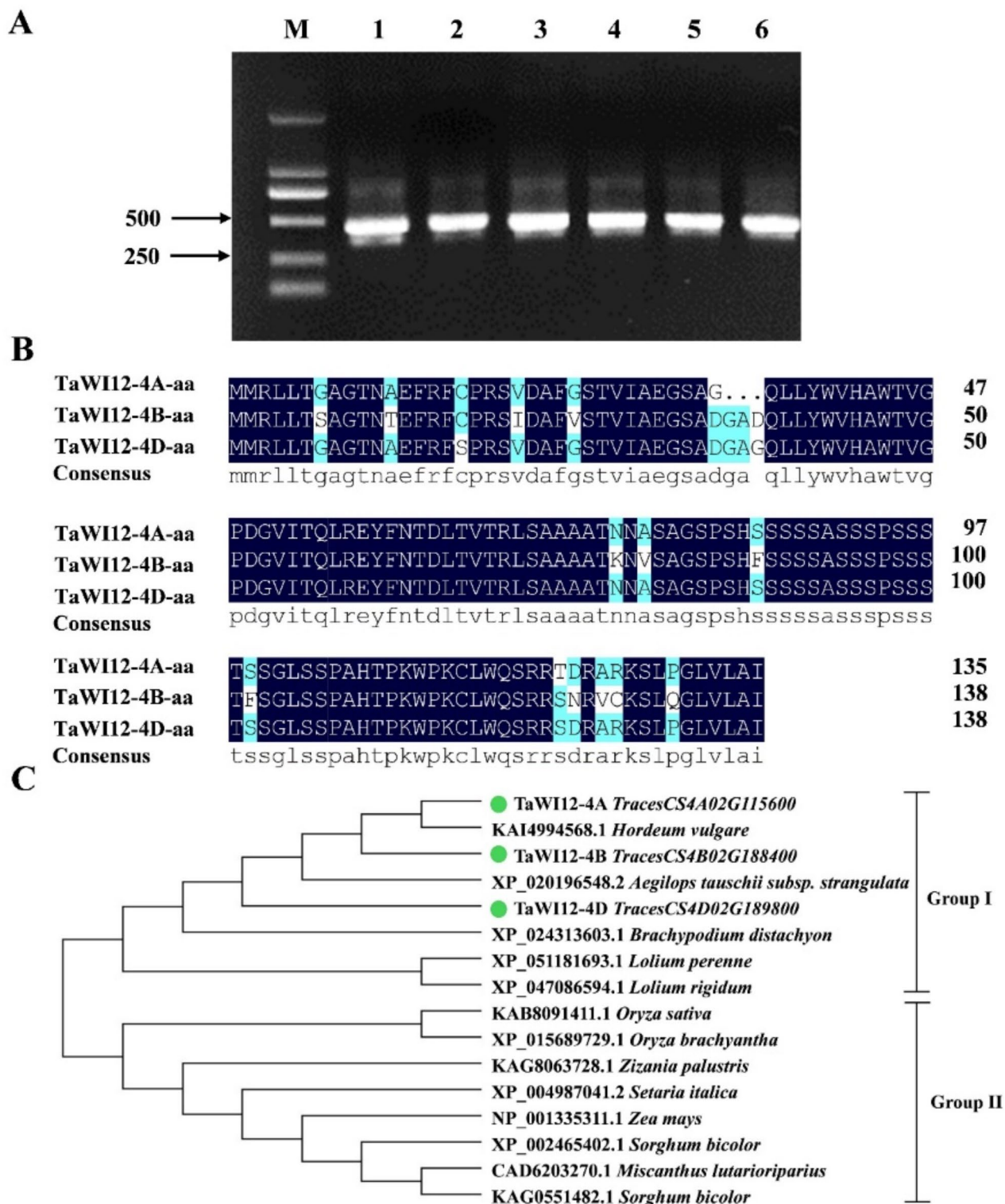


Fig. 2 PCR amplification, amino acid sequence comparison, and phylogenetic analysis of *TaWI12*. **(A)** PCR amplification of the *TaWI12* gene. M: DL2000 marker; 1–3: Amplification results of *TaWI12-4A*, *TaWI12-4B* and *TaWI12-4D* in CM28TP; 4–6: Amplification results of *TaWI12-4A*, *TaWI12-4B* and *TaWI12-4D* gene in HTS-1. **(B)** Amino acid sequence comparison of the *TaWI12*. **(C)** Maximum likelihood tree of the *TaWI12* protein from various plant species, with sequences retrieved from the NCBI protein database

Table 2 Computations of various physical and chemical parameters of TaWI12

	4A	4B	4D
Number of amino acids	135	138	138
Molecular weight	14215.90	14786.65	14429.03
Theoretical pI	9.88	9.30	9.85
Total number of negatively charged residues (Asp + Glu)	7	8	8
Total number of positively charged residues (Arg + Lys)	12	12	12
Formula	C ₆₁₉ H ₉₇₆ N ₁₈₂ O ₁₉₅ S ₄	C ₆₅₀ H ₁₀₁₈ N ₁₈₄ O ₂₀₁ S ₅	C ₆₂₇ H ₉₈₇ N ₁₈₅ O ₂₀₁ S ₃
The instability index (II)	44.06	47.71	47.06
Aliphatic index	70.22	74.28	69.42
Grand average of hydropathicity (GRAVY)	-0.179	-0.078	-0.214

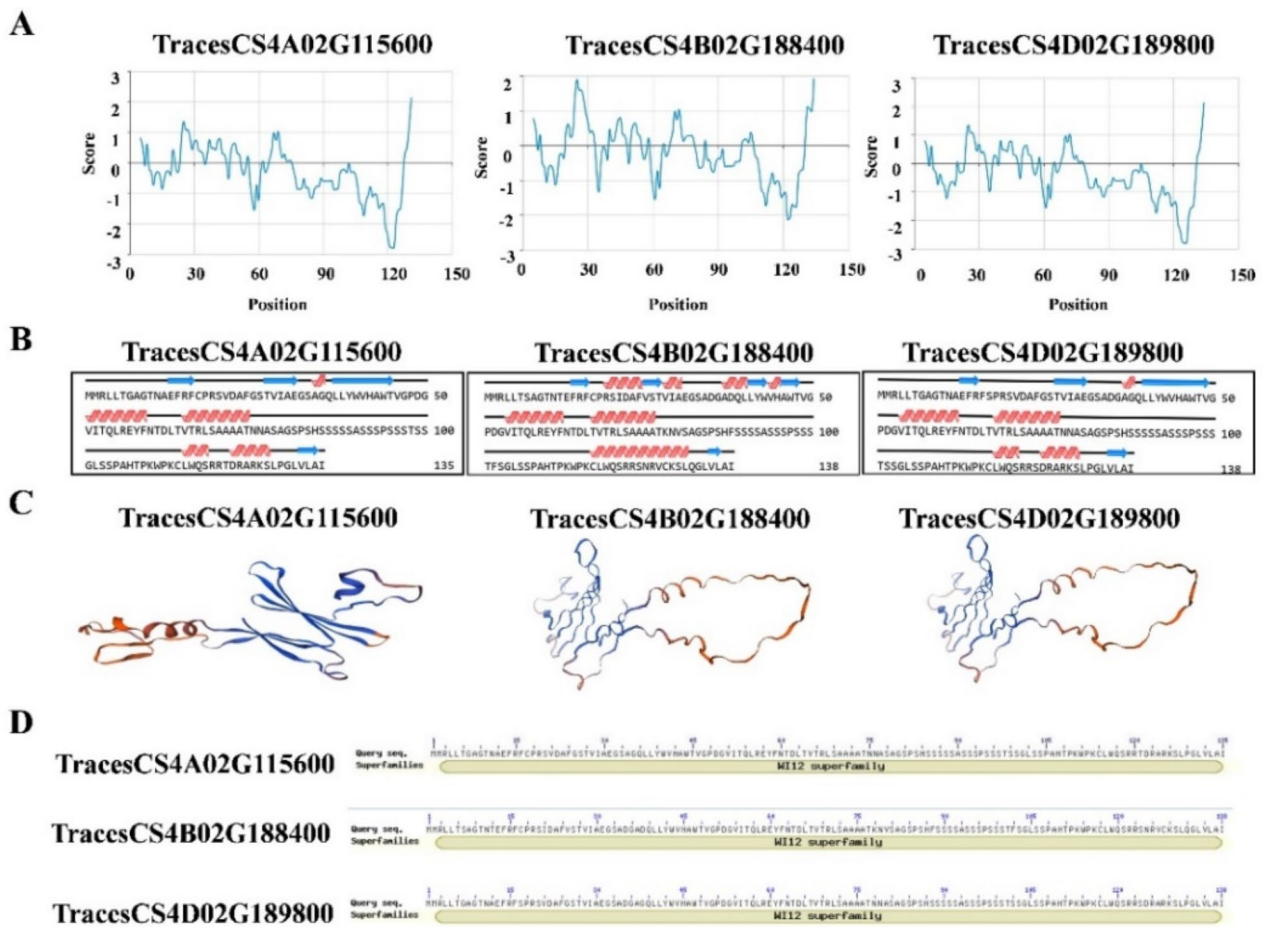


Fig. 3 Bioinformatics analysis of the TaWI12 protein. **(A)** Hydrophobicity profile of the TaWI12-4A, TaWI12-4B, and TaWI12-4D proteins. Note: The x-axis represents the sequence of amino acids encoding the protein, and the y-axis represents the hydrophilic and hydrophobic values. A value of 0 indicates a hydrophobic region, whereas a value of 0 indicates a hydrophilic region. **(B)** The predicted secondary proteins of TaWI12-4A, TaWI12-4B, and TaWI12-4D. Note: The red, blue, and black parts represent the alpha helix, β -extended strand, and random coil, respectively. **(C)** Tertiary structure prediction of the TaWI12-4A, TaWI12-4B, and TaWI12-4D proteins. **(D)** Conserved domain prediction of the TaWI12-4A, TaWI12-4B, and TaWI12-4D proteins

Table 3 Secondary structure of the TaWI12 protein

	4A	4B	4D
Alpha helix	20.74%	18.12%	16.67%
Extended strand	24.44%	24.64%	22.46%
Beta turn	5.93%	5.07%	7.25%
Random coil	48.89%	52.17%	53.62%

represent its function in wheat, given the differences in developmental contexts and genetic backgrounds.

Phenotypic analysis of TaWI12 in wheat edited by CRISPR/Cas9

To investigate the functional characterization of homologs of *TaWI12* in hexaploidy wheat, we generated

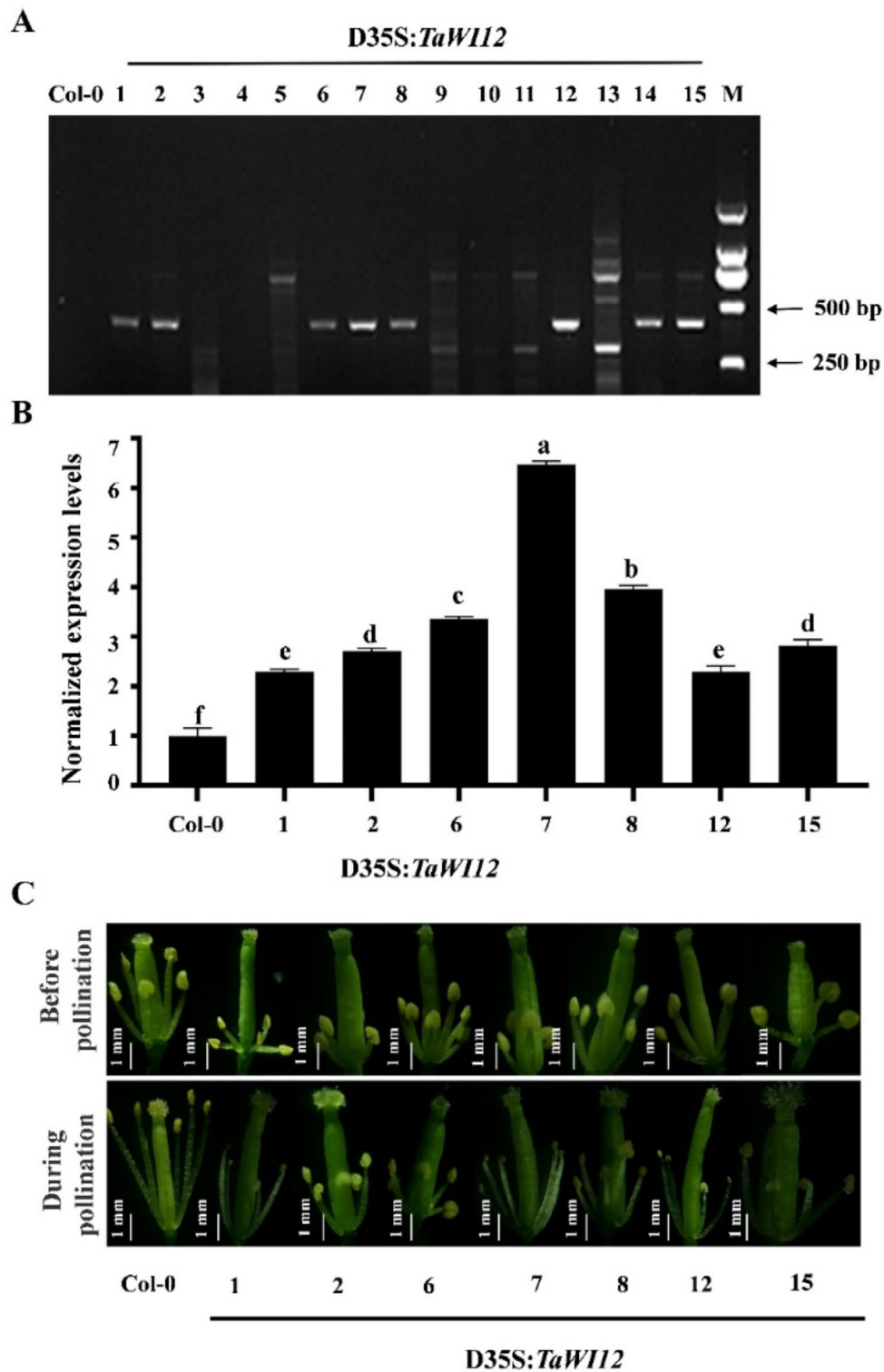


Fig. 4 Differences in the inflorescence phenotypes of Col-0 and transgenic *Arabidopsis* lines. **(A)**. 15 independent transgenic lines of the *TaW112* gene were detected via PCR. **(B)**. *TaW112* expression levels in 1, 2, 6, 7, 8, 12, and 15 leaves of the *TaW112* transgenic lines. *AtGAPDH* was used as the reference gene. **(C)**. Filament growth of transgenic *Arabidopsis* -1, -2, -6, -7, -8, -12, and -15 before and during pollination in the T₃ generation. Notes: The error bars represent the standard deviation (SD). Different letters indicate significant differences ($P < 0.05$), and the same letters indicate no significant differences ($P > 0.05$)

TaWII2 knockout mutants via the CRISPR-Cas9 technique in the wheat cultivar Fielder background. One construct, carrying both sgRNA1 and sgRNA2, was introduced into the WT via *Agrobacterium*-mediated transformation. The *TaWII2* genes in the A, B, and D subgenomes were validated through sequencing in the T₀ generation. Eventually, we successfully obtained 4 edited plants from *TaWII2-4A* and 4 edited plants from *TaWII2-4D*. However, no edited sites were detected in *TaWII2-4B* or in the coding region or promoter region.

We subsequently self-pollinated these T₀-edited plants to establish homozygous *TaWII2* knockout lines. Following the sequencing of editing sites in the T₁ generation plants, we successfully obtained homozygous editing materials on chromosomes A, D and AD (Fig. 5). On chromosome A, there are two edited homozygotes: ED10 and ED16. ED10 exhibited a 3 bp deletion, whereas ED16 featured a 5 bp deletion at the PAM site (Fig. 5A). For chromosome D, we also obtained two edited homozygotes: ED3 and ED20. ED3 displayed a 1 bp insertion, and ED20 had a 1 bp deletion at the PAM site (Fig. 5B). Furthermore, we also obtained two edited plants that were homozygous for chromosomes A and D: ED6 and ED15. ED6 displayed a 1 bp deletion on chromosome 4A and a 1 bp insertion on chromosome 4D. ED15 had a 1 bp deletion on the 4A chromosome and a 4 bp deletion on the 4D chromosome (Fig. 5C).

Phenotypic analysis was carried out on homozygous editing materials on chromosomes A, D and AD, including comparison of the morphological characteristics of pistils, stamens and leaves between T₁ knockout mutant plants and Fielder. Typically, Fielder's florets exhibit one pistil and three stamens, resulting in the production of one seed per floret. In contrast, the florets of ED3 and ED20 presented pistillody traits, with the most extreme manifestation being the homologous transformation of all three stamens into pistils; however, only a single seed was produced instead of the expected 2 to 4 seeds for each floret. Moreover, the florets of ED10, ED16, ED6, and ED15 did not exhibit pistillody (Fig. 6A-C). The expression of the *TaWII2* gene in pistillody stamens (EDPS) of ED20 and ED3 was analyzed via qRT-PCR. The expression levels of *TaWII2* in EDPS and EDP were significantly greater than those in FS, with an increase of more than 100-fold (Fig. 6D). We further analyzed the expression levels of the *TaWII2* gene in the spikes of edited plants. The results revealed that *TaWII2* was highly expressed in the spikes of ED3 and ED20, but the expression levels in the spikes of Fielder, ED10, ED16, ED6 and ED15 were slightly lower (Fig. 6F). Consequently, we hypothesize that editing of the promoter region did not inhibit the expression of the *TaWII2* gene but rather increased its expression of both ED20 and ED3. Upon further examination, we discovered a 1 bp deletion in ED20 and

a 1 bp insertion in ED3. These mutations occurred at the fourth base upstream of the PAM site in both gene editing lines (Fig. 5B). Consequently, we postulate that the deletion and insertion of 1 bp in the promoter region led to alterations in promoter activity, ultimately enhancing downstream gene expression. This may contribute to the development of pistillody stamen traits. In addition, we observed that the leaves of edited homozygous plants, including ED10, ED16, ED6, and ED15, exhibited varying degrees of cracking compared to those of Fielder. Notably, this cracking was not limited to the flag leaves; nearly all leaves of each mutant plant displayed this phenomenon. However, there was no leaf cracking in the edited homozygous plants at ED3 and ED20 (Fig. 6E). Therefore, we speculate that *TaWII2* may be involved in regulating pistillody and leaf cracking simultaneously.

Discussion

Wheat is a globally significant food crop that is extensively cultivated worldwide [39]. Multi-pistil wheat stands out as a valuable and rare resource for wheat breeding and the investigation of wheat flower development [40]. In this study, *TaWII2* was isolated from HTS-1 and CM28TP, and its sequences were compared and analyzed. The results revealed no disparity in *TaWII2* between HTS-1 and CM28TP, suggesting that the phenomenon of pistillody stamens might not be attributed to sequence differences but potentially linked to the differential expression of *TaWII2*. Bioinformatic analysis of *TaWII2* revealed that the protein is a member of the WII2 family.

The *TaWII2* gene may play a vital role in response to wounds

Plant cells are encapsulated by their rigid cell walls, which is a considerable challenge for wound healing in plant tissue. Cell-specific auxin accumulation occurs near plant wounds, and this increase in local auxin balances the rate of wound-induced cell expansion and restorative division in a dose-dependent manner [41]. Plants often transmit external signals into cells through interconnected signaling pathways, eventually activating defense responses by upregulating a range of defense-related genes in response to environmental stress [42]. In *Populus*, the expression of wound-inducible cDNA (*win4*) was examined in wounded leaves [43]. In maize, *GRMZM2G010909* encodes wound-induced protein 1, the expression of which is induced in response to mechanical wounding or pathogen attack [44]. In rubber trees, the dominance of hevein proteins is similar to that of wound-induced proteins. Hevein mRNA is frequently upregulated in leaves, stems, and latex derived from tapping stems in response to wounding or exogenous application of stress-related hormones such as ABA and ethylene [45].

A	<i>TaW112-4A</i>		
	PAM		
	GATC ACCAGCTCAGGGAGTACTTCAAC		Fielder
	GATC ACCAGC ---GGGAGTACTTCAAC	-3bp	ED10
	GATC ACCAGC -----GAGTACTTCAAC	-5bp	ED16
B	<i>TaW112-4D</i>		
	PAM		
	CAGCT CCAAGCTCAATCCATCGCCTCCA		Fielder
	CAGCT CCAAGCT CAATCCATCGCCTCCA	+1bp	ED3
	CAGCT CCAAGC -CAATCCATCGCCTCCA	-1bp	ED20
C	ED6		
	PAM		
	GATC ACCAGCTCAGGGAGTACTTCAAC		Fielder
	GATC ACCAGCT -AGGGAGTACTTCAAC	-1bp	<i>TaW112-4A</i>
	CAGCT CCAAGCTCAATCCATCGCCTCCA		Fielder
	CAGCT CCAAGCT CAATCCATCGCCTCCA	+1bp	<i>TaW112-4D</i>
	ED15		
	PAM		
	GATC ACCAGCTCAGGGAGTACTTCAAC		Fielder
	GATC ACCAGCT -AGGGAGTACTTCAAC	-1bp	<i>TaW112-4A</i>
CAGCT CCAAGCTCAATCCATCGCCTCCA		Fielder	
CAGCT CC -----TCAATCCATCGCCTCCA	-4bp	<i>TaW112-4D</i>	

Fig. 5 Genotyping of *TaW112* knockout lines generated via wheat gene editing in the T₁ generation. **(A)**. Editing on chromosome A. **(B)**. Editing on chromosome D. **(C)**. Editing chromosomes A and D. Note: The green letters, the red letters, the blue letters, and the dashed lines represent the PAM sequences, the sgRNA sequences, the nucleotide insertions, and the nucleotide deletions, respectively

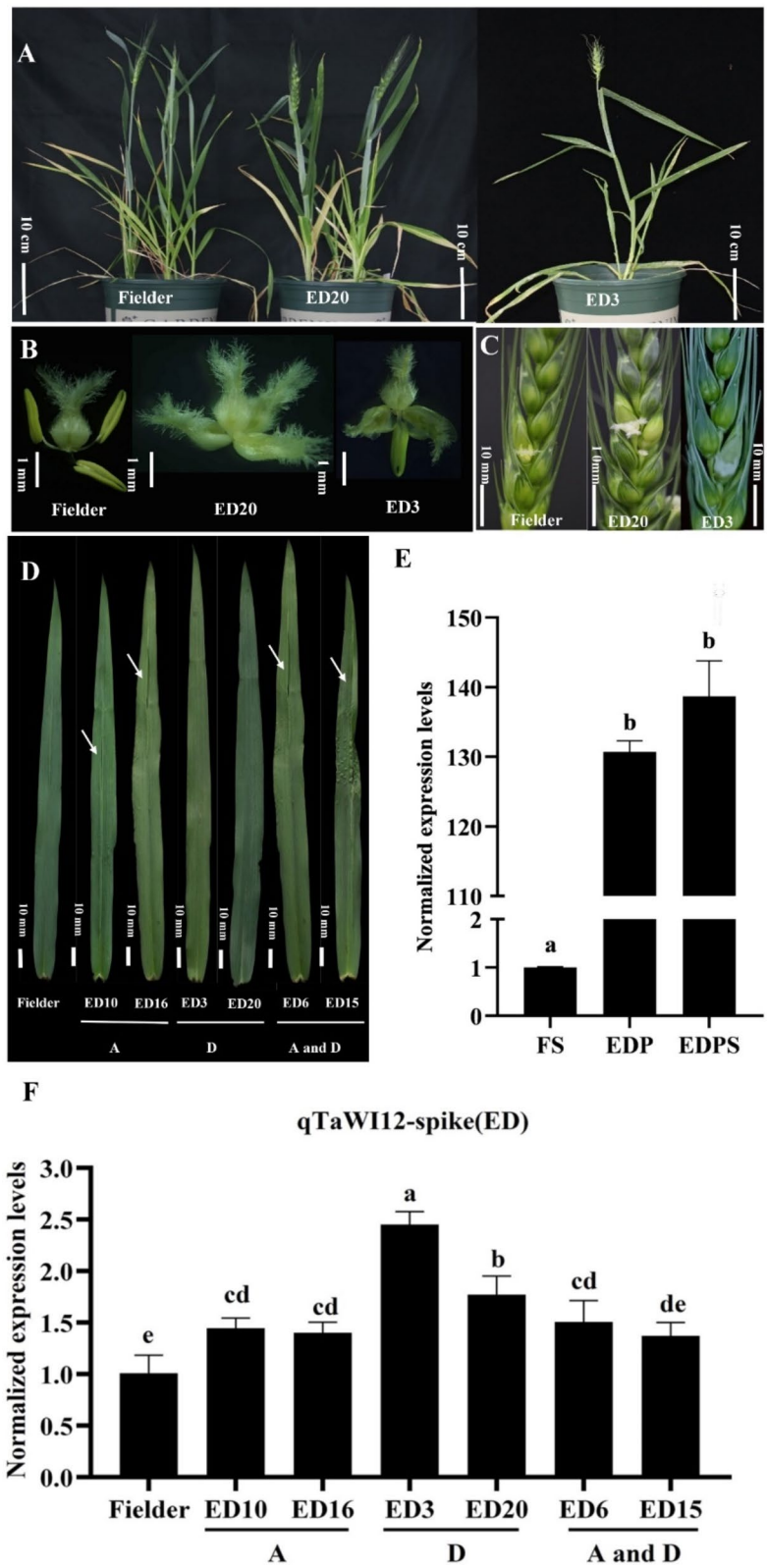


Fig. 6 (See legend on next page.)

(See figure on previous page.)

Fig. 6 Phenotype and expression analysis of Fielder and *TaW112* knockout lines in the T₁ generation. **(A)**. Plant phenotypes of Fielder and transgenic lines. **(B)**. Pistil and stamen phenotypes of Fielder and transgenic lines. **(C)**. Spike phenotypes of Fielder and transgenic lines. Note: P represents pistil; PS represents pistillody stamen; S represents stamen. **(D)**. Leaf phenotypes of Fielder and transgenic lines. Note: A represents homozygous editing on chromosome A; D represents homozygous editing on chromosome D; A and D represents homozygous editing on chromosomes A and D. The arrows represent leaf cracking. **(E)**. Expression of pistils and stamens in Fielder and transgenic lines. Note: FS represents a normal stamen; EDPS represents a pistillody stamen; EDP represents a pistil. **(F)**. Expression of spikes in Fielder and transgenic lines. The error bars represent the standard deviation (SD). Different letters indicate significant differences ($P < 0.05$), and the same letters indicate no significant differences ($P > 0.05$)

While research on the W112 family is limited, existing studies indicate that W112 family members are activated in plants in response to wounds, diseases and insect pests [23–25]. In this study, we observed a distinct leaf cracking phenotype in plants where *TaW112* was edited using CRISPR/Cas9. This phenomenon was evident in both homozygous mutants of the A genome and double homozygous mutants of the A and D genomes. We hypothesize that this phenotype may result from tissue damage caused by mechanical stress or pest/pathogen activity. In the absence of functional *TaW112*, the damaged tissues might be unable to heal properly, leading to the observed cracking. This hypothesis aligns with the potential role of *TaW112* suggested by prior studies. However, direct evidence linking the loss of *TaW112* function to impaired tissue repair is currently lacking. Further studies are needed to explore the molecular mechanisms underlying this phenotype and to validate this proposed connection.

Overexpression of *TaW112* could be the key factor contributing to the development of pistillody traits

Currently, there are few studies on the association between W112 and floral development. In *Mesembryanthemum crystallinum*, W112 is highly expressed in petals, styles, placenta, and seeds [22]. In rice, *LOC_Os05g27590*, which is associated with abiotic stress and cell wall defense, encodes the wound induced protein W112 and might participate in the cross-talk between pollination and stress responses [46]. Moreover, during the development and germination of rice pollen, 474 transcripts related to defense/stress response, including the wound-induced protein W112, were preferentially expressed in the pollen. These findings suggest that the capacity to handle abiotic and biotic stresses developed during pollen maturation may be critical for successful fertilization [8]. In this study, overexpression of the wheat *TaW112* gene in *Arabidopsis* revealed clear phenotypic alterations. Specifically, transgenic plants displayed shortened filaments relative to the stigma and variability in filament number, ranging from 2 to 6, compared to the wild type. These findings indicate that *TaW112* may influence stamen development, potentially causing abnormalities that disrupt floral organ structure. However, we recognize that these results primarily reflect the role of *TaW112* within the *Arabidopsis* system and may not directly represent its function in wheat due to the differing developmental and regulatory contexts between

these species. The overexpression experiments provide valuable insights into the potential effects of *TaW112*, but further studies in wheat are essential to validate its native role. To this end, our CRISPR/Cas9-mediated editing of *TaW112* in wheat demonstrated that specific promoter modifications, such as a 1 bp deletion or insertion upstream of the PAM site in the *TaW112-4D* promoter, led to pistillody traits. Interestingly, this deletion or insertion did not lead to a reduction in or inactivation of *TaW112* expression; instead, it resulted in the upregulation of *TaW112* expression in floret organs. We speculate that the deletion or insertion of the 4th base upstream of the editing site (PAM structure) in the promoter of *TaW112* on the 4D chromosome enhances promoter activity, thereby inducing the upregulation of *TaW112*. However, in the pistillody edited plants, each floret did not produce 2 to 4 seeds, which we speculated might have been caused by an incomplete pistillody. As a next step, we intend to overexpress this gene in wheat to further validate our hypothesis.

Conclusion

In this study, we successfully cloned *TaW112* from common wheat, and analyzed how the *TaW112* gene affects wheat development at the molecular level. To further explore the regulatory mechanism of the *TaW112* gene, we generated transgenic *Arabidopsis* and wheat plants. In *TaW112* knockout mutants, we observed different degrees of homologous conversion of stamens to pistils, as well as the occurrence of leaf cracking. We speculate that *TaW112* may be involved in response to wounds in wheat in addition to the development of pistils and stamens. We subsequently observed the healing response of WT and genetically edited plants to wounds by artificially wounding wheat leaves. In addition, we observed obvious filament shortening and decreasing in transgenic *Arabidopsis*. In further studies, an overexpression vector could be constructed for transformation into wheat to better study the function of *TaW112*. In summary, the results of this study hold significant theoretical value for research on leaf cracking, pistil and stamen development, and offer important application for high-yield breeding of wheat.

Abbreviations

HTS-1	Homologous transformation sterility-1
TP	Three-pistil mutants
FS	The normal stamens of Fielder

EDPS Pistillody stamens of edited homozygous plants
EDP Pistils of edited homozygous plants
ORFs Open reading frames

Author contributions

Yuhuan Guo, and Yan Zhang: Investigation, Data curation, Formal analysis, Writing – original draft, Writing – review & editing, Visualization. Yuhao Li: Investigation, Data curation, Formal analysis. Yichao Wu and Mingli Liao: Validation, Writing – review & editing. Zhongsong Peng: Resources. Yonghong Zhou: Writing – review & editing. Zaijun Yang: Writing – review & editing, Funding acquisition.

Funding

This study was supported by the National Natural Science Foundation of China (Grant No. 32272066, 32060456), and the Natural Science Foundation of Sichuan Province (Grant No. 2025ZNSFSC0156).

Data availability

The nucleotide sequence and protein sequence of the *TaWI12* gene on chromosomes A, B, and D (TraesCS4A02G115600, TraesCS4B02G188400, and TraesCS4D02G189800) were obtained through the WheatOmics 1.0 website (<http://202.194.139.32>) and the website is open to all researchers. All supporting data for this manuscript are included in the manuscript and its additional files.

Declarations

Ethics approval and consent to participate
not applicable.

Consent for publication
not applicable.

Competing interests
The authors declare no competing interests.

Clinical trial number
not applicable.

Received: 24 October 2024 / Accepted: 21 January 2025

Published online: 29 January 2025

References

- Carlsson J, Leino M, Sohlberg J, et al. Mitochondrial regulation of flower development [J]. *Mitochondrion*. 2008;8(1):74–86. <https://doi.org/10.1016/j.mito.2007.09.006>.
- Al-Gburi SAH, Al-Gburi BKH. Improving the nutritional content of wheat grains by integrated weeds management strategies and spraying with nanomicro-nutrients [J]. *J Saudi Soc Agricultural Sci*. 2023;23(1):88–92. <https://doi.org/10.1016/j.jssas.2023.09.005>.
- Qiu YL, Chen HQ, Zhang SX, et al. Development of a wheat material with improved bread-making quality by overexpressing *HMW-GS 1Sx2.3** from *Aegilops longissima* [J]. *Crop J*. 2022;10(6):1717–26. <https://doi.org/10.1016/j.cj.2022.04.001>.
- United Nations. (2019) World Population Prospects 2019: Highlights. In: Statistical Papers - United Nations (Ser. A), Population and Vital Statistics Report (Vol. ST/ESA/SER.A/423).
- Le Bourgot C, Liu XX, Buffière C, et al. Development of a protein food based on texturized wheat proteins, with high protein digestibility and improved lysine content [J]. *Food Res Int*. 2023;170:112978. <https://doi.org/10.1016/j.foodres.2023.112978>.
- Irshad A, Guo HJ, Ur Rehman S, et al. Induction of semi-dwarf trait to a three pistil tall mutant through breeding with increased grain numbers in wheat [J]. *Front Genet*. 2022;13:828866. <https://doi.org/10.3389/fgene.2022.828866>.
- Duan ZB, Shen CC, Li QY, et al. Identification of a novel male sterile wheat mutant *dms* conferring dwarf status and multi-pistils [J]. *J Integr Agric*. 2015;14(9):1706–14. [https://doi.org/10.1016/S2095-3119\(14\)60936-9](https://doi.org/10.1016/S2095-3119(14)60936-9).
- Li Z, Ma SC, Liu D, et al. Morphological and proteomic analysis of young spikes reveals new insights into the formation of multiple-pistil wheat [J]. *Plant Sci*. 2020;296:110503. <https://doi.org/10.1016/j.plantsci.2020.110503>.
- Yamamoto N, Chen ZY, Guo YH, et al. Gene co-expression modules behind the three-pistil formation in wheat [J]. *Funct Integr Genom*. 2023;23(2):123. <https://doi.org/10.1007/s10142-023-01052-w>.
- Peng ZS. A new mutation in wheat producing three pistils in a floret [J]. *J Agron Crop Sci*. 2003;189(4):270–2. <https://doi.org/10.1046/j.1439-037X.2003.00040.x>.
- Zhu XX, Ni YJ, He RS, et al. Genetic mapping and expressivity of a wheat multi-pistil gene in mutant *127P* [J]. *J Integr Agric*. 2019;18(3):532–8. [https://doi.org/10.1016/S2095-3119\(18\)61935-5](https://doi.org/10.1016/S2095-3119(18)61935-5).
- Guo JL, Zhang GS, Song YL, et al. Comparative transcriptome profiling of multi-ovary wheat under heterogeneous cytoplasm suppression [J]. *Sci Rep*. 2019;9(1):8301. <https://doi.org/10.1038/s41598-019-43277-5>.
- Mahlandt A, Rawat N, Leonard J, et al. High-resolution mapping of the *Mov-1* locus in wheat by combining radiation hybrid (RH) and recombination-based mapping approaches [J]. *Theor Appl Genet*. 2021;134(7):2303–14. <https://doi.org/10.1007/s00122-021-03827-w>.
- Wang ZG, Xu DH, Ji J, et al. Genetic analysis and molecular markers associated with multi-gynoecia (*Mg*) gene in Trigrain wheat [J]. *Can J Plant Sci*. 2009;89:845–50. <https://doi.org/10.4141/CJPS09022>.
- Peng ZS, Yang ZJ, Ouyang ZM, et al. Characterization of a novel pistillody mutant in common wheat [J]. *Aust J Crop Sci*. 2013;7(1):159–64. <https://doi.org/10.3316/informit.143085142306594>.
- Liang YS, Gong JY, Yan YX, et al. Fine mapping and candidate-gene analysis of an open glume multi-pistil 3 (*mp3*) in rice (*Oryza sativa* L.) [J]. *Agriculture*. 2022;12(10):1731. <https://doi.org/10.3390/agriculture12101731>.
- Liu XG, Kim YJ, Müller R, et al. *AGAMOUS* terminates floral stem cell maintenance in *Arabidopsis* by directly repressing *WUSCHEL* through recruitment of Polycomb Group proteins [J]. *Plant Cell*. 2011;23(10):3654–70. <https://doi.org/10.1105/tpc.111.091538>.
- Pautler M, Eveland AL, LaRue T, et al. *FASCIATED EAR4* encodes a bZIP transcription factor that regulates shoot meristem size in maize [J]. *Plant Cell*. 2015;27(1):104–20. <https://doi.org/10.1105/tpc.114.132506>.
- Mahfud M, Murti RH. Inheritance pattern of fruit color and shape in multi-pistil and purple tomato crossing [J]. *AGRIVITA J Agricultural Sci*. 2020;42(3):572–83. <https://doi.org/10.17503/agrivita.v42i3.2515>.
- Yang Q, Yang ZJ, Tang HF, et al. High-density genetic map construction and mapping of the homologous transformation sterility gene (*hts*) in wheat using GBS markers [J]. *BMC Plant Biol*. 2018;18(1):301. <https://doi.org/10.1186/s12870-018-1532-x>.
- Stanford A, Bevan M, Northcote D. Differential expression within a family of novel wound-induced genes in potato [J]. *Mol Gen Genet MGG*. 1989;215:200–8. <https://doi.org/10.1007/BF00339718>.
- Yen SK, Chung MC, Chen PC, et al. Environmental and developmental regulation of the wound-induced cell wall protein WI12 in the halophyte ice plant [J]. *Plant Physiol*. 2001;127(2):517–28. <https://doi.org/10.1104/pp.010205>.
- Guo W, Zhang F, Bao AL, et al. The soybean *Rhg1* amino acid transporter gene alters glutamate homeostasis and jasmonic acid-induced resistance to soybean cyst nematode [J]. *Mol Plant Pathol*. 2019;20(2):270–86. <https://doi.org/10.1111/mpp.12753>.
- Zhang LQ, Huang X, He CY, et al. Novel fungal pathogenicity and leaf defense strategies are revealed by simultaneous transcriptome analysis of *Colletotrichum fructicola* and strawberry infected by this fungus [J]. *Front Plant Sci*. 2018;9:434. <https://doi.org/10.3389/fpls.2018.00434>.
- Lv WT, Du B, Shanguan XX, et al. BAC and RNA sequencing reveal the brown planthopper resistance gene *BPH15* in a recombination cold spot that mediates a unique defense mechanism [J]. *BMC Genomics*. 2014;15(1):674. <https://doi.org/10.1186/1471-2164-15-674>.
- Sperotto RA, de Araújo Junior AT, Adamski JM, et al. Deep RNAseq indicates protective mechanisms of cold-tolerant *indica* rice plants during early vegetative stage [J]. *Plant Cell Rep*. 2018;37(2):347–75. <https://doi.org/10.1007/s00299-017-2234-9>.
- Hao XY, Tang H, Wang B, et al. Integrative transcriptional and metabolic analyses provide insights into cold spell response mechanisms in young shoots of the tea plant [J]. *Tree Physiol*. 2018;38(11):1655–71. <https://doi.org/10.1093/triephys/tpy038>.
- Zheng XT, Yu ZC, Peng XF, et al. Endogenous ascorbic acid delays ethylene-induced leaf senescence in *Arabidopsis thaliana* [J]. *Photosynthetic*. 2020;58(3):720–31. <https://doi.org/10.32615/ps.2020.028>.

29. Yang ZJ, Peng ZS, Yang H, et al. Suppression subtractive hybridization identified differentially expressed genes in pistil mutations in wheat [J]. *Plant Mol Biology Report*. 2011;29:431–9. <https://doi.org/10.1007/s11105-010-0249-2>.
30. Yao FQ, Li XH, Wang H, et al. Down-expression of *TaPIN1s* increases the tiller number and grain yield in wheat [J]. *BMC Plant Biol*. 2021;21:1–11. <https://doi.org/10.1186/s12870-021-03217-w>.
31. Waddington SR, Cartwright PM, Wall PC. A quantitative scale of spike initial and pistil development in barley and wheat [J]. *Ann Botany*. 1983;51(1):119–30. <https://doi.org/10.1093/oxfordjournals.aob.a086434>.
32. Zhao Y, Ai XH, Wang MC, et al. A putative pyruvate transporter *TaBASS2* positively regulates salinity tolerance in wheat via modulation of *ABI4* expression [J]. *BMC Plant Biol*. 2016;16:1–12. <https://doi.org/10.1186/s12870-016-0795-3>.
33. An G. Binary ti vectors for plant transformation and promoter analysis [M]. *Methods in enzymology*. Acad Press. 1987;153:292–305. [https://doi.org/10.1016/0076-6879\(87\)53060-9](https://doi.org/10.1016/0076-6879(87)53060-9).
34. Clough SJ, Bent AF. Floral dip: a simplified method for *Agrobacterium*-mediated transformation of *Arabidopsis thaliana* [J]. *Plant J*. 1998;16(6):735–43. <https://doi.org/10.1046/j.1365-313x.1998.00343.x>.
35. Sun QX, Qu J p, YuY., et al. *TaEPFL1*, an EPIDERMAL PATTERNING FACTOR-LIKE (EPFL) secreted peptide gene, is required for stamen development in wheat [J]. *Genetica*. 2019;147:121–30. <https://doi.org/10.1007/s10709-019-00061-7>.
36. Schmittgen TD, Livak KJ. Analyzing real-time PCR data by the comparative CT method [J]. *Nat Protocols*. 2008;3(6):1101–8. <https://doi.org/10.1038/nprot.2008.73>.
37. Cheng M, Fry JE, Pang S, et al. Genetic transformation of wheat mediated by *Agrobacterium tumefaciens* [J]. *Plant Physiol*. 1997;115(3):971–80. <https://doi.org/10.1104/pp.115.3.971>.
38. Yamamoto N, Xiang GL, Tong W, et al. Over-expression of a plant-type phosphoenolpyruvate carboxylase derails *Arabidopsis* stamen formation [J]. *Gene*. 2024;927(15):148749. <https://doi.org/10.1016/j.gene.2024.148749>.
39. Zajączkowska U, Denisow B, Łotocka B, et al. Spikelet movements, anther extrusion and pollen production in wheat cultivars with contrasting tendencies to cleistogamy [J]. *BMC Plant Biol*. 2021;21(1):136. <https://doi.org/10.1186/s12870-021-02917-7>.
40. Yu ZY, Luo Q, Peng ZS, et al. Genetic mapping of the three-pistil gene *Pis1* in an F₂ population derived from a synthetic hexaploid wheat using multiple molecular marker systems [J]. *Cereal Res Commun*. 2021;49:31–6. <https://doi.org/10.1007/s42976-020-00078-1>.
41. Hoermayer L, Montesinos JC, Marhava P et al. (2020) Wounding-induced changes in cellular pressure and localized auxin signaling spatially coordinate restorative divisions in roots [J]. *Proceedings of the National Academy of Sciences of the United States of America*, 117(26): 15322–15331. <https://doi.org/10.1073/pnas.2003346117>
42. Chung KM, Sano H. Transactivation of wound-responsive genes containing the core sequence of the auxin-responsive element by a wound-induced protein kinase-activated transcription factor in tobacco plants [J]. *Plant Mol Biol*. 2007;65(6):763–73. <https://doi.org/10.1007/s11103-007-9240-1>.
43. Davis JM, Egelkrout EE, Coleman GD, et al. A family of wound-induced genes in *Populus* shares common features with genes encoding vegetative storage proteins [J]. *Plant Mol Biol*. 1993;23(1):135–43. <https://doi.org/10.1007/BF00021426>.
44. Kebede AZ, Johnston A, Schneiderman D, et al. Transcriptome profiling of two maize inbreds with distinct responses to Gibberella ear rot disease to identify candidate resistance genes [J]. *BMC Genomics*. 2018;19(1):131. <https://doi.org/10.1186/s12864-018-4513-4>.
45. Broekaert I, Lee HI, Kush A, et al. Wound-induced accumulation of mRNA containing a hevein sequence in laticifers of rubber tree (*Hevea brasiliensis*) [J]. *Proc Natl Acad Sci USA*. 1990;87(19):7633–7. <https://doi.org/10.1073/pnas.87.19.7633>.
46. Li MN, Xu WY, Yang WQ, et al. Genome-wide gene expression profiling reveals conserved and novel molecular functions of the stigma in rice [J]. *Plant Physiol*. 2007;144(4):1797–812. <https://doi.org/10.1104/pp.107.101600>.

Publisher's note

Springer Nature remains neutral with regard to jurisdictional claims in published maps and institutional affiliations.